Sequential Homo-Interpenetrating Polymer Networks of Poly(2-hydroxyethyl methacrylate): Synthesis, Characterization, and Calcium Uptake

Traian V. Chirila,[1,2,3,4] Karina A. George,[1,5,6] Wael A. Abdul Ghafor,[2,7] Steven J. Pas,[8,9] Anita J. Hill[8,10]

[1]*Queensland Eye Institute, 41 Annerley Road, South Brisbane, Queensland 4101, Australia*
[2]*Australian Institute for Bioengineering and Nanotechnology, University of Queensland, St Lucia, Queensland 4072, Australia*
[3]*Faculty of Health Sciences, University of Queensland, Herston, Queensland 4006, Australia*
[4]*Discipline of Chemistry, Faculty of Science and Technology, Queensland University of Technology, Brisbane, Queensland 4001, Australia*
[5]*Discipline of Medical Sciences, Faculty of Science and Technology, Queensland University of Technology, Brisbane, Queensland 4001, Australia*
[6]*Institute of Health and Biomedical Innovation, Queensland University of Technology, Kelvin Grove, Queensland 4059, Australia*
[7]*Centre for Advanced Imaging, University of Queensland, St Lucia, Queensland 4072, Australia*
[8]*CSIRO, Materials Science and Engineering, Clayton 3168, Victoria, Australia*
[9]*Department of Materials Science and Engineering, Monash University, Clayton 3168, Victoria, Australia*
[10]*School of Chemistry, Monash University, Clayton 3168, Victoria, Australia*

Received 13 November 2011; accepted 15 January 2012
DOI 10.1002/app.36824
Published online in Wiley Online Library (wileyonlinelibrary.com).

ABSTRACT: Formation of homo-interpenetrating polymer networks (homo-IPNs) of poly(2-hydroxyethyl methacrylate) (PHEMA) and their capacity for calcification are investigated. A sequential method is established to generate IPNs of rank I and II, containing two or three crosslinked networks. Although the networks are chemically identical, thermo-mechanical analysis (DSC, DMA) suggests some phase separation. Calcification of PHEMA hydrogels, thought to be controlled by the free volume pathways accessible to calcium ions, is investigated by positron annihilation lifetime spectroscopy (PALS) and experimental calcium deposition. While calcium uptake is reduced in IPNs, the size of the free volume elements estimated by PALS remain constant at radii of 2.6 Å (dry) and 2.9 Å (hydrated), both in PHEMA and IPNs. The reduction of calcium uptake cannot be therefore associated with the size reduction of the angstrom-size free volume elements detectable by PALS, and is attributed to the effect of chain packing on pores too large to be detected by PALS. © 2012 Wiley Periodicals, Inc. J Appl Polym Sci 000: 000–000, 2012

Key words: interpenetrating networks (IPN); hydrogels; PHEMA; glass transition; PALS; calcification

INTRODUCTION

There is no ambiguity in the definition of an interpenetrating polymer network (IPN), or a sequential IPN, or a homo-IPN.[1–6] Briefly, an IPN is a combination of two polymeric networks, where at least one network (designated as network II) was generated and/or crosslinked in the presence of the other network (network I), while a sequential IPN results when the crosslinked network I is swollen to an equilibrium with monomer II, which is subsequently polymerized (with or without a crosslinking agent) to generate network II. If the networks I and II are identical, the resulting IPN is known as a sequential homo-IPN. If the diffusion of monomer II into network I does not proceed to completion, the result is a gradient IPN, where obviously the composition or crosslink density varies according to location throughout the polymer mass. An IPN can be made, in theory, from an unlimited number of networks generated in succession.

Materials that in today's terminology would be qualified as IPNs or sequential IPNs have been actually reported prior to Hermann Staudinger's revolutionary (and correct) hypothesis[7–9] on the true nature of polymers. Such compositions have been claimed by Aylsworth in a patent application[10] (lodged in 1910 and published in 1914), where

Correspondence to: T. V. Chirila (traian.chirila@qei.org.au).

Contract grant sponsors: Prevent Blindness Foundation, Queensland, Australia (Viertel's Vision Program), Australian Research Council.

networks I and II were, respectively, vulcanized rubber and phenol-formaldehyde resins. Later, sequential homo-IPNs of polystyrene[11] and poly(methyl methacrylate)[12] have been reported, but it is not clear whether any of the networks were crosslinked. The first to describe true sequential homo-IPNs was Johann Staudinger in a series of patents,[13–15] where the crosslinked networks were polystyrene or poly(methyl methacrylate). (According to some sources,[3,4] Johann Staudinger was Hermann's son, an assumption we were unable to confirm). The aim of these patents was to produce strain- and void-free polymeric materials, and a careful examination reveals that some of the disclosed homo-IPNs consisted of multiple networks resulting from up to five successive swelling/polymerization cycles.

Millar's seminal study[16] in 1960 on homo-IPNs of polystyrene crosslinked with divinylbenzene is important for at least two reasons: it not only introduced the term IPN as such, but also marked a more scientific approach to the investigation of the homo-IPNs (which are still known alternatively as "Millar IPNs"). It was followed, over the next two decades, by only three notable articles[17–19] dedicated also to the homo-IPNs based on polystyrene, and the results of these studies have been thoroughly analyzed by Sperling.[1] Against the intuitive, but naive, opinion that the sequential homo-IPNs are homogeneous materials where network I is indistinguishable from network II or any other successive networks, and consequently the properties of the IPNs should be the same as those of the parent network, these studies demonstrated the contrary. Generally, the network I had the lowest density and tensile or shear moduli, which all increased as the number of the successive networks increased, while the swelling behaviour followed an opposite trend. Despite some discrepancy between results, this was attributed to the existence of internetwork entanglements (additional physical entanglements, in fact) and to the predominance of network I due to its greater continuity in space as compared to the subsequent networks.

We are investigating sequential homo-IPNs of poly(2-hydroxyethyl methacrylate), henceforth PHEMA, a hydrogel used as a biomedical polymer in ophthalmology. At the present time, there are two ocular implants made from PHEMA available on the medical market: an artificial cornea,[20,21] and an orbital enucleation implant.[22,23] In both devices, the salient feature is a joint between two constitutive elements—a transparent PHEMA hydrogel and a PHEMA sponge—through the formation of gradient homo-IPNs. However, to generate sequential homo-IPNs of PHEMA is challenging because PHEMA does not swell in its own monomer, 2-hydroxyethyl methacrylate (HEMA). Therefore, compounds that are miscible with HEMA and also can function as swelling agents for PHEMA must be used in the preparation of monomer mixtures, to enable penetration into the parent network. In the case of PHEMA/HEMA system, water and certain alcohols are obviously the main candidates to fulfil such requirements. Indeed, water has been the medium of choice in the manufacture of the devices mentioned above.[24,25] Long durations must be allowed for the diffusion of the HEMA monomer mixture into the PHEMA parent network, otherwise the level of interpenetration of network II into network I is too low for practical purposes.[26]

In light of further applications of PHEMA as an ophthalmic biomaterial, we have previously proposed that excessive chain packing may occur in its homo-IPNs, leading to a reduction of the free volume available for the penetration of the calcium ion and its partner anions (phosphate, carbonate), and our preliminary results[27] appeared to support this hypothesis. The reduction of calcium uptake by hydrogels is not a trivial matter, as their calcification can be a serious drawback in the ophthalmic applications. There is considerable clinical evidence that spoliation of hydrogels, both on the surface and internally, with deposits comprised from calcium salts (frequently accompanied by lipids and proteins) leads to loss of transparency of contact lenses,[28] artificial intraocular lenses,[29] and artificial corneas,[30] and to possible pathological complications.

In the present study, we investigated sequential homo-IPNs of PHEMA generated from two and, respectively, three networks. A methodology to generate these IPNs was established, and the products were characterized by physical methods, including positron annihilation lifetime spectroscopy (PALS), differential scanning calorimetry (DSC), and dynamic mechanical analysis (DMA). The calcium uptake was also comparatively measured in the homopolymer PHEMA and its two IPNs.

OBSERVATIONS ON NOMENCLATURE

The nomenclature of the IPNs, especially of those containing more than two networks, has been generally arbitrary and diverse, and consensus in usage was met only incidentally. Millar[16] used the term "primary polymer" for the network I, and "secondary intermeshed copolymer" and "tertiary intermeshed copolymer" for the IPN containing two and three networks, respectively. Other authors[31–34] used the terms "two-component" or "three-component" IPNs to denote the number of chemically different polymers incorporated in an IPN, rather than the number of successively generated networks. Accordingly, the homo-IPNs are "one-component" IPNs regardless of how many successive networks they may comprise. Unaware of this, we have used the same terminology to describe homo-IPNs of PHEMA

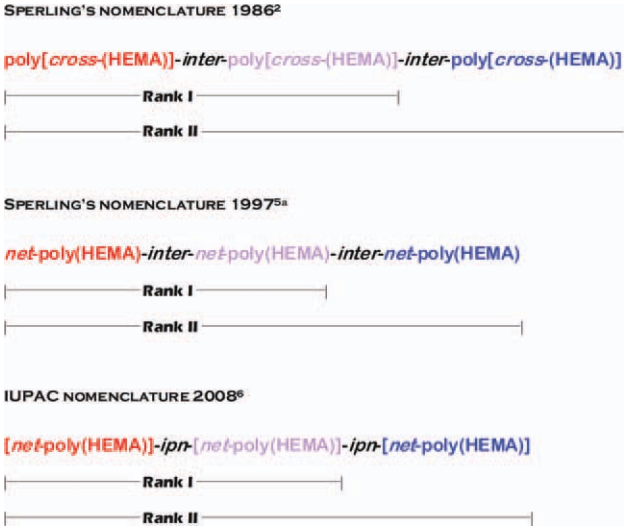

Scheme 1 Proposed naming of the IPNs comprising successive networks, and integration with various styles of nomenclature. [Color figure can be viewed in the online issue, which is available at wileyonlinelibrary.com.]

comprising a number of successive networks;[35] for instance, a "three-component" IPN was made by swelling the parent network in HEMA, polymerizing, then swelling the resulting material in HEMA, and again polymerizing. It contains three networks but only one chemically identifiable polymer (PHEMA).

We propose now the term "IPN of rank *N*" to be used for naming the sequential IPNs, where *N* represents the number of networks generated onto the parent network through successive swelling/polymerization cycles. An IPN of rank I (henceforth IPN-I) will consist of two networks (parent network I and network II), rank II (henceforth IPN-II) of three networks, and so on. Scheme 1 illustrates this concept and also shows its correlation to some of the nomenclature styles employed for IPNs.

EXPERIMENTAL

Materials

2-Hydroxyethyl methacrylate (HEMA) and ethylene dimethacrylate (EDMA) were supplied by Bimax Chemicals, USA, with certified purities of 99.3% and 99.9%, respectively, and used as received. The initiators 2,2′-azo-*bis*(2,4-dimethyl valeronitrile) (V-65) and 2,2′-azo-*bis*(2-methylpropionamide) dihydrochloride (V-50) were supplied by Wako Chemical Industries, Japan, the latter being a water-soluble cationic initiator. Sodium chloride, potassium chloride, dipotassium hydrogen orthophosphate, hydrochloric acid 32%, and petroleum spirit (b. r. 40–60°C) were all supplied as UNIVAR analytical reagents by Ajax Finechem, Australia. Calcium chloride dihydrate, dichloromethane, absolute methanol, and *tris*(hydroxymethyl)aminomethane (TRIS) were supplied by Sigma-Aldrich, USA. Calcium carbonate was supplied as an analytical reagent by Chem-Supply, Australia. A ready-made aqueous solution of 70% nitric acid was supplied by Labscan Asia, Thailand, as Lab-Scan™ analytical reagent. Water used in all experiments was supplied by Merck KGaA, Germany, as water for chromatography (Lichrosolv®). Throughout this report, all percentage concentration or composition values were expressed by weight (w/w), unless otherwise specified.

Preparation of IPNs

Parent network (PHEMA)

Network I was produced by thermally initiated bulk homopolymerization of HEMA. A mixture of monomer, 0.5% EDMA and 0.1% V-65 was placed in polypropylene moulds fitted in the cavities of a specially designed two-piece aluminium moulding unit. After evacuating the air with a laboratory water-jet pump and replacing it with nitrogen, the sealed unit was placed in a controlled-temperature water bath and maintained for 50 h while a temperature program was run from 30 to 70°C. After cooling the mould, the PHEMA cylindrical buttons were removed and conditioned at 110°C for 12 h in an oven. The buttons were further lathe-machined into disks of approximately 7 mm in diameter and 2 mm in thickness, which were then polished with the polishing diamond compound grade 1-KD-C1 (Kemet International, UK). The polished disks were ultrasonicated in a bath in petroleum spirit for 10 min and dichloromethane for 5 min, thoroughly rinsed in petroleum spirit again, and dried in an oven at 80°C for 8 h. The disks were extracted with water in a Soxhlet apparatus for 70 h, and then dried, first in an oven at 110°C for 8 h, followed by 24 h at 50°C in a vacuum oven. They were each weighed on an analytical balance and stored in individually labelled screw-capped glass containers. About one hundred disks were produced for this study.

IPN-I

HEMA was mixed with 0.35% EDMA to generate component "A". Component "B" was prepared by dissolving V-50 (0.1% to monomer) in a mixture of water and methanol. Components "A" and "B" were then mixed thoroughly, assuring that the final weight proportion of HEMA/water/methanol was 70/20/10, and portions of 5 to 7 mL were added to the individual containers in order to submerge each of the disks selected to fulfil the role of network I in the IPN. The containers were kept in a refrigerator for 3 to 4 weeks, until the disks became fully swollen. This can be easily seen by visual examination,

as the swelling front advanced towards the centres of the disks. The swollen disks were gently blotted with lint-free tissue, placed on aluminium foil and kept in an oven at 70°C for 24 h, and then at 100°C for 3 h. Further processing followed the protocol described for PHEMA (the parent network), including extraction, drying in two stages, weighing and storing in capped labelled containers. The IPN-I and IPN-II disks were not subjected to lathe-cutting or polishing.

IPN-II

The penetrating monomer solution for generating IPN-II was the same as that described above for IPN-I, with the difference that the weight proportion of HEMA/water/methanol was 75/20/5. The resulting disks were processed according to a protocol identical to that for the IPN-I disks.

Weight gain

The weight gain was calculated as the ratio of the dry weight acquired by a sample after the formation of IPN (i.e., the sum of network I and IPN-I or, respectively, of network I, IPN-I and IPN-II) to the initial dry weight of the same sample prior to its incorporation into IPNs as the network I. Equation (1) and (2) were used, where $W_{d,H}$ is the dry weight of the homopolymer specimen prior to further swelling and polymerization; $W_{d,\mathrm{I}}$ is the dry weight of the IPN-I specimen; and $W_{d,\mathrm{II}}$ is the dry weight of the IPN-II specimen, both IPNs starting from the same homopolymer.

$$(\text{wt. gain})_{\mathrm{I}} = W_{d,\mathrm{I}}/W_{d,\mathrm{H}} \quad (1)$$

$$(\text{wt. gain})_{\mathrm{II}} = W_{d,\mathrm{II}}/W_{d,\mathrm{H}} \quad (2)$$

We have measured the weight gain in IPN-I for 30 samples, and the weight gain in IPN-II for 15 samples.

Equilibrium water content

Three samples of each PHEMA, IPN-I, and IPN-II, all dried and weighed according to the protocols described above, were submerged in water in their respective containers. The samples were kept in water for 18 days. Throughout this period, the water was replaced four times with fresh water. During the last 3 days, the constancy of weight was checked by repeated weighing. The equilibrium water content (EWC) was calculated with the classic formula:

$$\mathrm{EWC} = (W_w - W_d)/W_x \times 100\ (\%) \quad (3)$$

where W_w and W_d are the weights of a fully hydrated (wet) disk and, respectively, of the same disk before hydration (dry).

Density

Density of the dry polymer samples was measured using a gas displacement pycnometer (Accupyc 1330, Micromeritics, USA). The mass of each sample was measured on a four-digit microbalance (Sartorius R160P, Germany). The average density and population standard deviations were calculated from five measurements made at 22°C using helium to determine the sample volume.

Differential scanning calorimetry

The analysis was performed using a Mettler Toledo DSC1 STAR^e System (Mettler Toledo, USA & Switzerland) calorimeter. The samples were sealed in aluminium pans, and the measurements were performed under continuous purge of high-purity nitrogen. To measure the reversible thermal transitions, the samples were subjected to a thermal cycle consisting of first heating from room temperature up to 100°C, then cooling down to −100°C, followed by heating up to 160°C, both at a rate of 10°C/min. The glass transition temperature was taken as the midpoint of the slop change in the heat flow versus temperature plot.

Dynamic mechanical analysis

The analysis was performed using a Mettler Toledo DMA/STDA861^e STAR^e System (Mettler Toledo, USA & Switzerland) dynamic mechanical analyzer, from −100 to 160°C at various frequencies and a heating rate of 3°C/min. The measurements were carried out in the shear mode for cylindrical samples with a geometry factor of 22.7 m^{-1}. The shear moduli and the loss tangent (dissipation factor) were measured as a function of temperature.

Positron annihilation lifetime spectroscopy

The PALS measurements on both dry and hydrated samples were conducted in an automated EG&G Ortec Fast-Fast Coincidence System (USA). The measurements were performed at ambient temperature with a timing resolution of 240 ps. A thin (2.54 μm), sealed Mylar® envelope containing radioactive isotope ^{22}Na was used as the positron source. The envelope was sandwiched between two PHEMA (or two IPNs) samples (as disks). To dissipate the electronic charge build-up from ionization of the material, the disks-source sandwich was wrapped in aluminium foil. At least five spectra of 10^6 integrated counts were collected for each sample and analyzed using the LT9 program.[36] This program is based on a finite-term model and fits positron and positronium (Ps) lifetime data to a sum of three decaying

exponential components (i.e., three lifetimes). The shortest and intermediate lifetimes are characteristic of para-positronium (*p*-Ps) self-annihilation and of free and trapped positron annihilations, respectively. The *p*-Ps self-annihilation lifetime is fixed at 0.125 ns, and the free and trapped positron annihilation lifetimes are between 0.35 and 0.45 ns. The longest lifetime (τ_{oPs}) is attributed to ortho-positronium (*o*-Ps) and used to characterize the free volume of samples.[37]

Calcification assay

To prepare the calcifying medium, a TRIS buffer solution (0.05*M*) was first prepared by dissolving 8 g NaCl, 0.2 g KCl and 6 g TRIS base in 800 mL water, adjusting the pH to 7.4 by the addition of HCl, and then adding water to make 1 L solution. In this amount of buffer solution, 1.135 g (7.72 mmol) $CaCl_2{\cdot}2H_2O$ were dissolved to obtain solution A. Separately, 0.8047 g (4.62 mmol) K_2HPO_4 were dissolved in another litre of TRIS buffer to obtain solution B. Just before starting the calcification experiments, equal volumes of solutions A and B were mixed together to provide enough amount for submerging completely all samples in their individually labelled containers.

Four samples of each PHEMA, IPN-I, and IPN-II were hydrated to equilibrium according to the protocol described above. After discarding the water used for hydration, about 5 mL of calcifying medium was added to each container. The containers were mounted on a shaker (Multi Reax, Heidolph Instruments GmbH, Germany) and shaken at 800 rpm for 5 weeks at room temperature. On the second and fourth week, the existing medium was replaced in each container with fresh calcifying medium.

Each calcified disk was removed from its container, gently and uniformly rinsed in a slow stream of water, and placed in a silica crucible. All twelve crucibles were placed in a temperature-programmable furnace (Modutemp Furnaces, Australia), slowly heated to 500°C, ashed at 700°C for 1 h, and then allowed to cool down overnight. The white residues on the bottom of the crucibles were dissolved by adding 10 mL HNO_3 70% in each crucible and the resulting solutions were transferred to individual 25-mL volumetric flasks and diluted to mark with water. These solutions were then analyzed by inductively coupled plasma emission spectroscopy (ICP-OES) in a Varian VISTA-MPX CCD Simultaneous ICP-OES instrument, using the Ca emission line at 317.933 nm, a plasma power of 1.25 kW and a plasma argon flow of 13.5 L/min. For calibration, solutions were prepared by dissolving precisely weighed amounts of $CaCO_3$ in 10 mL HNO_3 70% and diluting to 25 mL in volumetric flasks. The background medium was also analyzed as a solution of 10 mL HNO_3 70% diluted to 25 mL, and this signal was subtracted from the analyte signals.

The results of the ICP analysis were processed by the one-way analysis of variance (ANOVA) in conjunction with the Tukey's Post Hoc multiple comparison test, using the SPSS 16.0 software.

TABLE I
Weight Gain and Equilibrium Water Content in the Parent Network (PHEMA) and the Homo-IPNs

Sample	Weight gain[a]	EWC (%)
PHEMA	1	36.90 ± 0.27 ($N = 3$)
IPN-I	1.87 ± 0.09 ($N = 30$)	35.15 ± 0.35 ($N = 3$)
IPN-II	3.36 ± 0.16 ($N = 15$)	32.52 ± 0.43 ($N = 3$)

[a] The results are given as mean values ± SD, rounded to two decimal places.

RESULTS AND DISCUSSION

Synthesis of IPNs

We established a general method to obtain sequential homo-IPNs of PHEMA, which differs to some extent from the methods we have reported in a previous study.[27] The penetration of monomer into network I and again into the IPN-I was assured by using as solvent a mixture of water and methanol. It was critical to allow the complete swelling of the networks at a low temperature (refrigerator); although it took considerable time, this stage was necessary to avoid premature polymerization. To establish the ideal HEMA/water/methanol proportions, a number of trials were needed to find a compromise where the water amount did not prevent the full dissolution of the hydrophobic crosslinking agent (EDMA) but was sufficient to ensure that the swelling process would not require a too long duration, since unexpected polymerization may take place even in refrigerating conditions if an initiator is present. The ideal amount of methanol, necessary to accelerate the swelling process and to enhance the solubility of EDMA, had also to be found by trial, considering that too much methanol can cause cracks in the material upon swelling.

Weight gain and EWC

The obtained experimental values (Table I) for these two parameters clearly suggested the formation of IPNs. As additional networks were packed into the parent network, the weight gain increased while the EWC decreased. The trend in the evolution of EWC is identical to that found by Millar for the "toluene regain" in the polystyrene and its IPNs of rank I and II.[16]

TABLE II
Density Values of the Parent Network (PHEMA) and the Homo-IPNs measured in Their Dry State

Sample	Density (g/cm^3)[a]
PHEMA	1.221 ± 0.002 ($N = 5$)
IPN-I	1.249 ± 0.001 ($N = 5$)
IPN-II	1.245 ± 0.002 ($N = 5$)

[a] The results are given as mean values ± SD, rounded to three decimal places.

Density

The measured densities are given in Table II, including the population standard deviations. The IPNs have a higher density than the parent network; however, an increase in the rank of the IPNs, i. e. additional chain packing, had no effect on the density of the polymers in a dry state. The finding is in partial disagreement with Millar's results,[16] where the density increased monotonically with the rank of polystyrene IPNs.

Glass transition

Notwithstanding its importance for characterization of amorphous and semicrystalline polymers, the glass transition temperature (T_g) is notoriously difficult to determine as a true constant for a given polymer.[38] This aspect is clearly illustrated in Table III, which—*albeit* not comprehensive—presents a relevant compilation of the literature regarding the T_g values reported for PHEMA[39–64] over the last five decades. The experimental values are sensitive to a multitude of factors such as the time scale of measurements, imprecise definitions for T_g, presence of contaminants or crystalline phases, variations in the synthetic procedure, and—especially—the type of method used to measure it.

The mobility of main macromolecular chains and of the shorter side chains in amorphous polymers is a crucial determinant of their physical properties.[47,65–68] Molecular mobility depends unequivocally upon temperature: the rise in temperature can trigger certain modes of chain motion, while its decrease leads to the "freezing-in" of certain motions. These events, which are related to energy absorption, are known as "transitions," "relaxations," or "dispersions." The transition regions detectable in glass-forming amorphous polymers through a number of methods—especially dielectric spectroscopy, DMA or DSC—are traditionally labeled as α, β, γ, δ, etc. from the higher to the lower temperature (i.e., $T_\alpha > T_\beta > T_\gamma > T_\delta > ...$).[47,65–76] It should be mentioned that transitions occurring at temperatures lower than T_γ have been seldom reported.

The α-transition is caused by the activation of micro-Brownian motion of large segments in the main chain, which acquire significant mobility leading to large-scale conformational rearrangements, and is considered a "primary relaxation." It is related to the transition from the glassy to the rubbery state, and consequently T_α is customarily used as a measure for T_g. The other transitions, all occurring at lower temperatures, are regarded as "secondary relaxations," for which various underlying molecular mechanisms have been proposed. Thus, the β-transition is attributed either to the motion of short segments of the main chain (in polymers without side chains) or to the rotation of pendant side groups around the bond linking each of them to the

TABLE III
A Literature Survey of the Experimental T_g Values for PHEMA

T_g (°C)	Method	Reference
55	Dilatometry	39
86	Linear expansion and torsion measurements	40
98	Dilatometry	41
93.5	DMA[a]	42
88[b]	DMA	43
94[c]	DMA	43
110–111	DMA	44
103	DMA[d]	45
74	DSC[e]	46
103	DMA	47
115–126	DSC	48
50.3	Calculated	49
98	DSC	50
87	DSC	51
109	DMA	51
108	DSC	52
70	DSC	53
109	DSC	54
75–110	DSC	55
113–114	DSC	56
105	DMA[d]	57
133	DMA[f]	58
56	DSC	58
99	DSC	59
~ 102	DSC, DMA[f]	60
56	DSC[g]	61
60	DSC[h]	61
133	DMA[f,g]	61
145	DMA[f,h]	61
88.2	DSC	62
110	DSC	63
112	DSC	64
120	DMA	64

[a] Dynamic mechanical analysis.
[b] At low crosslinking.
[c] At high crosslinking.
[d] From the loss modulus peak.
[e] Differential scanning calorimetry.
[f] From the tan δ peak.
[g] Polymer made by photopolymerization.
[h] Polymer made by thermal polymerization.

main chain (in substituted polymers). In the case of poly(alkyl methacrylates), β-transition can be caused by the rotation of methyl groups or/and by that of the whole —COOR groups. The γ-transition is due to motions within the side group itself. In poly(alkyl methacrylates), for instance, this relaxation can be generated by the hindered motion of the groups R within the —COOR side chains. In the particular case of PHEMA (homopolymer), various T_α, T_β, and T_γ have been reported, respectively, such as: 110–111°C, 30°C, and −125°C;[44] 103°C, 27°C, and −133°C;[47] 100°C, 20°C, and −120°C.[74] A review of the transitions in PHEMA is also available.[77]

In the polymeric multicomponent systems, such as blends and IPNs, a single T_g is detectable if the components are miscible and form one phase. If they are not miscible, a T_g for each phase will be observed. Between these two extremes, distinct T_g values will be observed, but the more miscible the components, the closer these values.[5] The merging of differing T_g values in IPNs may also be accelerated by increasing the crosslinking density in either network.[78] Another effect in the multicomponent systems is the broadening of T_g signal, which was attributed both to a wide distribution of the segmental motion rates for each component and to intrinsic differences in the motional rate between components.[79] In brief, the occurrence of a single T_g in an IPN can be taken as a proof of the homogeneity of the system; however, the temperature interval of the α-transition is usually broad and may even become extremely wide.

The IPNs of PHEMA with synthetic polymers have been produced previously and investigated episodically with an aim of improving the properties of the parent polymer for biomedical applications. Thus, a number of studies were dedicated to IPNs of PHEMA where the second components were polyurethanes,[58,61,80–84] poly(ε-caprolactone) (PCL),[85–89] acrylic polymers,[90–93] polystyrene,[94,95] poly(vinyl alcohol),[96] or other polymers.[97–101] The systems described were all bicomponent, either full IPNs (sequential or simultaneous) or semi-IPNs (with PHEMA being either the crosslinked component or the linear one), and their thermal and/or dynamic mechanical behaviour have been investigated in some of these studies.[58,61,81,83–88,90,94,96,98] In general, the formation of IPNs from PHEMA and hydrophobic polymers led to phase-separated systems,[58,61,81,84,85,87,88,90,94] illustrated in excessive broadening of the signals in both DSC and DMA plots, and/or the existence of two values for the T_g in the DSC plots and the occurrence of two peaks in the tan δ (the loss tangent) plots (DMA). Nevertheless, an apparently miscible sequential IPN has been reported between PHEMA and a polyurethane made from modified castor oil and hexamethylene diisocyanate, which displayed only a single value for T_g (DSC).[83] Also, based on the occurrence of a single T_g (DSC), phase separation was discounted in the only reported IPN of PHEMA with another hydroxyl-bearing hydrophilic polymer, poly(vinyl alcohol).[96]

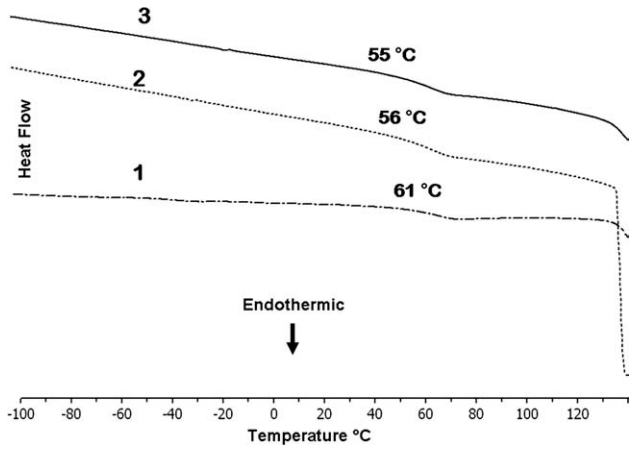

Figure 1 DSC thermograms of the parent network PHEMA (1), IPN-I (2), and IPN-II (3).

A common feature of all previous studies was the broad range of the reported T_g values. For instance, in a semi-IPN of PHEMA (as the uncrosslinked component) and a polyurethane, the values of T_g corresponding to PHEMA component were between 48 and 56°C as determined by DSC and between 110 and 133°C as estimated from the tan δ plots.[58] In a subsequent report,[81] the same system was investigated by combined DSC analysis and laser-interferometric creep rate spectroscopy (CRS). It was found that, virtually, the T_g of the system ranged from −60°C to +160°C. This enormous spread was tentatively attributed to an anomalous dynamic behaviour explained by a "constraining segmental dynamics" induced by additional covalent linkages due to late chemical reaction between residual isocyanate groups and the hydroxyl groups in the PHEMA component. This process may have led to the heterogeneity of segmental dynamics within each T_g.

In our present study, the DSC analysis revealed one transition attributable to T_g, situated within a very broad range (38 to 105°C) (Figure 1), with midpoint temperatures recorded by the instrument at 61°C (PHEMA), 56°C (IPN-I) and 55°C (IPN-II). No other transitions were observed. The endothermic deflection starting around 130°C (and extending beyond 160°C; not shown in the figure) can be attributed to the vaporization of the non-freezing bound water, which could not be removed from samples by conventional drying. It is known[102–104] that this type of water is strongly bound to the hydrophilic groups in natural or synthetic polymers and is retained up to temperatures well beyond 100°C, being removed completely in the range 130–170°C. This was confirmed in PHEMA by an endothermic deflection in

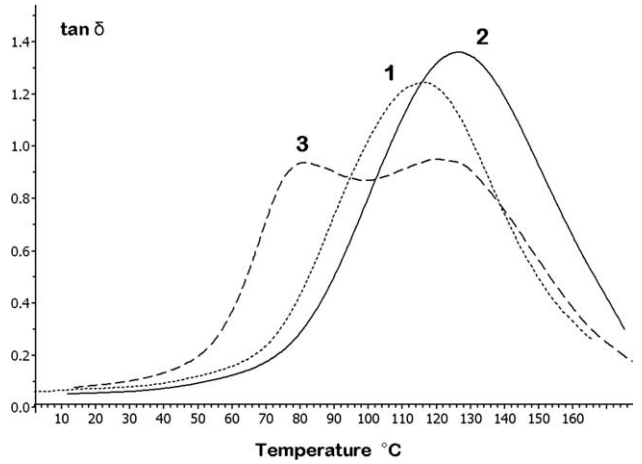

Figure 2 The tan δ versus temperature plots of the parent network PHEMA (1), IPN-I (2), and IPN-II (3). The frequency was 5 Hz.

the DSC thermogram extending beyond 120°C,[56] and by the differential thermal analysis (DTA) thermogram indicating that vaporization of bound nonfreezing water takes place between 130 and 175°C, with a peak around 160°C.[105]

A single value for the T_g is usually interpreted as proof of miscibility between the IPN components, however the shift of T_g to lower values in the IPNs and the broadness of signals may suggest a certain level of phase separation.

The DMA analysis revealed a slightly more complicated scenario. The most informative were the plots tan δ versus temperature (Figure 2). No β- or γ-transitions could be detected at lower temperatures. While PHEMA showed an α-transition in the interval 100 to 128°C, with a midpoint value at 115°C, and the IPN of rank I displayed also a single transition between 115 and 137°C, with a midpoint value at 125°C, the IPN of rank II showed two very broad signals at 81°C (interval 74 to 92°C) and at 120°C (interval 107 to 134°C), respectively. As the splitting of tan δ signal has been usually considered a proof for phase separation in multicomponent polymer systems, including the IPNs based on PHEMA,[58,61,90,94] we have to conclude that the homogeneity of the PHEMA homo-IPNs investigated here may be compromised as the rank of successive networking is increased. Indeed, we demonstrated previously,[20] by using transmission electron microscopy (TEM), that the gradient homo-IPNs of PHEMA presented a discontinuous morphology due to phase segregation, which was attributed to the fact that the first network to be synthesized (the parent network) controls the morphology of the IPN, and to the existence of microregions differing in segment and crosslinking density.

Estimation of free volume size by PALS

The lifetime of *o*-Ps, τ_{oPs}, is longer in larger free volume elements and is used to characterize the free volume element size.[37] In this study, the τ_{oPs} values were converted to effective free volume element sizes using a semiempirical model based on a spherical free volume geometry:[106–108]

$$\tau_{oPs} = \frac{1}{2}\left[1 - \frac{R}{R+\Delta R} + \frac{1}{2\pi}\sin\left(\frac{2\pi R}{R+\Delta R}\right)\right]^{-1} \quad (4)$$

where τ_{oPs} (in ns) is the lifetime of the *o*-Ps , R is the free volume element radius (in Å), and ΔR is the electron layer thickness, which is set to 1.66 Å.[106,109] Table IV gives the PALS measurement data and the estimated average free volume element radii for both dry and hydrated polymers. There was no difference between the free volume measured in the parent network and that measured in the IPNs. The free volume size increased due to hydration.

Calcium uptake in hydrogels

Generally, all synthetic polymers can undergo dystrophic calcification when in contact with living tissues. This process is known as biomaterial-associated calcification and leads to the deposition of calcium salts phases (commonly phosphates) on the polymer itself and/or the host tissue. The deposits are usually of an apatitic nature. While the polymers that do not have affinity for water are preferentially calcified at the interface, those able to absorb water and swell to form hydrogels can undergo calcification both at the interface and inside the material. As mentioned, the biomaterial-associated

TABLE IV
PALS Data and Free Volume Radii for the Parent Network (PHEMA) and the Homo-IPNs

Sample	τ_{oPs} (ns)[a] Dry	F.V. radius (Å)[b] Dry	τ_{oPs} (ns) Hydrated	F.V. radius (Å)[c] Hydrated
PHEMA	1.73 ± 0.01 ($N = 5$)	2.6	2.05 ± 0.01 ($N = 5$)	2.9
IPN-I	1.72 ± 0.01 ($N = 5$)	2.6	2.05 ± 0.01 ($N = 5$)	2.9
IPN-II	1.72 ± 0.01 ($N = 5$)	2.6	2.04 ± 0.01 ($N = 5$)	2.9

[a] The results for the lifetime of *o*-Ps are given as mean values ± SD, rounded to two decimal places.
[b] F.V., free volume.
[c] The values derived for the free volume element radii were rounded to one decimal place.

calcification of hydrogels is a major cause for their failure as biomaterials for ocular devices.

The contact of hydrogels with living tissues is not a prerequisite for the calcification of these materials, which can be easily achieved also in abiogenic conditions by using a variety of metastable calcifying solutions. The *in vitro* calcification shows all characteristics of a spontaneous process based on mechanisms yet to be elucidated. Calcification of PHEMA, a widely used biomaterial, has been rather extensively investigated, but mainly restricted to the study of the subcutaneous or intramuscular implants in experimental animals or to the examination of failed prosthetic devices after their retrieval from human patients. The *in vitro* calcification of PHEMA has been studied to a lesser extent.[110–118] Some of our own previous investigations suggested that enhanced local supersaturation within the polymer network due to salting-out solute effects,[119] and the presence of diffusion gradients[120] may contribute to triggering nucleation and crystal growth of calcium phosphate phases. Consequently, it was implied[121] that the abiogenic calcification of synthetic hydrogels may have, after all, a level of complexity not much lower that that of the calcification of typical biogenic substrata, such as collagen. Further, we have found that the amount of calcium phosphate deposited *in vitro* inside PHEMA was reduced in its sequential homo-IPN of rank I by 58 to 75%.[27] This finding was rationalized then in terms of the reduction of the size of unoccupied free volume available for penetration and transport of calcium and phosphate ions due to redundant molecular (chain) packing through the formation of IPNs.

An aim of the present study was to examine more closely the above assertion, working in conditions that differed to some extent from the previous study. While a calcifying medium resulting from $CaCl_2$ and Na_3PO_4 has been used previously,[27] in the experiments reported here we used a calcifying metastable solution[122,123] of a composition closer to that of the physiologic fluids and with a buffering that can be better controlled. As mentioned before, the method to generate the IPNs was also different from the methods described previously.[27] We evaluated in the present study the effect of redundant chain packing on calcification not only in the sequential homo-IPN of rank I but also in that of rank II.

The results of the calcification assay are given in Table V, showing that all samples investigated underwent calcification when subjected to the conditions in our experimental assay. In each of the IPN-I and IPN-II there was a statistically significant quantitative reduction of the calcium uptake, as compared to the parent network, of about 39 and 43% respectively. This reduction was less than previously reported,[27] likely a consequence of different experimental conditions. There was no statistically significant difference between the amount of calcium measured in IPN-I and IPN-II, showing that an increase in the rank of successive networks (which is equivalent to additional chain packing), does not reduce further the penetration and uptake of calcium ions. Clearly, our previous suggestion[27] needs reassessment. First, the reduction of the *size* of accessible free volume is not the only event that can be expected when IPNs are generated. After all, such reduction should not be expected at all, as the size of the free volume is strictly controlled by the existence of van der Waals forces and therefore it cannot be lowered beyond a certain limit, an aspect that we have overlooked in the previous report.[27] Second, an efficient chain packing may occur in an IPN due to energetically favoured chain alignments, with the consequence that the concentration, not the size, of the free volume elements can be reduced. The fewer the available free volume elements, the fewer the calcium ions that can globally be accommodated into material.

TABLE V
Calcium Content in PHEMA and Homo-IPNs Determined by ICP Emission Spectroscopy

Sample	Calcium content [mg Ca (g polymer)$^{-1}$][a]
PHEMA	2.37 ± 0.33 ($N = 4$)
IPN-I	1.44 ± 0.13 ($N = 4$)
IPN-II	1.34 ± 0.28 ($N = 4$)

[a] The results are given as mean values ± SD, rounded to two decimal places. Tukey's multiple comparison test in conjunction with ANOVA indicated statistically significant differences between PHEMA and IPN-I ($P = 0.002$) and between PHEMA and IPN-II ($P = 0.001$), but no significant difference between IPN-I and IPN-II ($P > 0.5$).

Our PALS analysis resulted in values for the *o*-Ps lifetimes (free volume element radii) and intensities (related to the concentration of free volume elements) which do not significantly differ between the parent network and IPN-I or IPN-II, when compared within the dry and, respectively, hydrated states. This means that the values measured for the range of free volume that can be probed by the *o*-Ps cannot explain the reduction of calcium uptake. Indeed, there are limits to the probing capability of *o*-Ps; for instance, PALS cannot detect free volume elements that are too small (radius <1.9 Å), or too large (radius >15 nm), or are oscillating too rapidly.[124] The values of the average free volume radii determined in the present study indicate that the hydrated Ca^{2+} ion (the effective radius of the ion with its first hydration shell is about 6 Å) would be too large anyway to penetrate through the free volume elements of the size detected by PALS, if the ions are transported through the free volume with their hydration shell. The hydrated ion transport process in polymers may depend specifically on a certain

fraction of the unoccupied/accessible volume, and PALS estimation of the free volume element size is relevant to the process being investigated only if the values measured represent the portion of the unoccupied volume which is the controlling factor for that particular process.[109] Obviously, the angstrom-size free volume elements detected by PALS are not the controlling factor over the transport of calcium and phosphate ions in these hydrogels.

It remains that the reduction of calcium uptake in the IPNs, when compared with that in the parent polymer network, must be related to the existence of pores too large to be detected as free volume by PALS. Indeed, by using nuclear magnetic resonance (^{1}H-NMR) spectroscopy,[125,126] we found previously in the hydrated PHEMA three distinct ranges of pore size, as indicated by the three components of the spin-spin relaxation time (T_2), which were situated in the nanometre and micrometre regions, the largest corresponding to water pockets and cracks. Complementary techniques such as PALS[54,126] and ^{129}Xe NMR spectroscopy[126] have also revealed in PHEMA pore size ranges in the sub-nanometre region. Obviously, there are many avenues for extraneous ions to penetrate into PHEMA, but most of these are outside of the probing limits of the *o*-Ps. A reduction in the penetration of calcium ions into, and transport through, the PHEMA networks (homopolymer or IPNs) appears thus to be related to the changes in the nanometre and/or micrometre pores, rather than those in the angstrom-size free volume elements. The former are the types of pores that can indeed be affected by the redundant molecular packing due to the formation of IPNs, unlike the latter, which are stabilized and unchangeable due to the existence of van der Waals forces.

The total detected porosity will contribute to the measured density. Although the redundant chain packing does not affect the sub-nanometre pores, the densities of IPN-I and IPN-II are greater than that of the parent network. This result suggests a reduction in the size of the pores in the nanometre and micrometre regions, which are undetectable by PALS. The similarity between the densities of IPN-I and IPN-II is in agreement with the measured calcium uptakes.

Our results and conclusions are consistent with other recent studies on ion and water transport in hydrogels. Similar conclusions were reached by other investigators[127,128] with respect to the transport of salt (NaCl) in phase-separated crosslinked poly(ethylene oxide) hydrogels. These authors indicated that phase-separated films generally had more open structures than homogeneous films, and in their case the former contained large internal pores (from 30 nm to 1 μm), such that the transport of water and salt in these pores may be by convective flow. They concluded that the pore size and density, rather than the free volume, would primarily control the transport properties in their phase-separated hydrogels.

CONCLUSIONS

The sequential homo-IPNs of PHEMA are difficult to make because PHEMA does not absorb, and swell into, its progenitor monomer HEMA. We demonstrated that by mixing HEMA with agents (water, alcohols) able to swell PHEMA, the synthesis of homo-IPNs is possible.

Although the components in these homo-IPNs are chemically identical, phase separation occurs to a certain extent, a finding that confirms previous reports.

The size of free volume elements in the angstrom range, as measured by PALS, proved to be constant regardless of the redundant chain packing attained through successive networking. Therefore, the reduction of calcium uptake in the IPNs cannot be correlated to the free volume, but with the existence of nanometre- and micrometre-size pockets, which are outside of the detection range of PALS. However, we believe that the generation of IPNs remains a valid procedure of reducing the calcium deposition on/into hydrogels, which is of interest when the hydrogels are used as biomaterials for ophthalmic applications.

AUTHOR CONTRIBUTIONS

T.V.C. conceived the frame of the study, designed the experiments, carried out the synthesis of polymers, performed the weight gain and EWC measurements and processed the data, and wrote the paper; K.A.G. carried out the calcification assay, coordinated the ICP analysis, and assisted to the interpretation of results; W.A.A.G. performed the thermomechanical evaluation and processed and interpreted the data; S.J.P. carried out the density and PALS measurements and processed the data; A.J.H. designed the PALS analytical procedures, coordinated the PALS measurements and interpreted the results, and wrote sections of the paper.

The authors are indebted to William Kwiecien (Queensland University of Technology, Brisbane, Australia) for expert assistance in performing the ICP analysis. AJH thanks to the CSIRO for support through the OCE Science Australia Leader scheme.
This article is dedicated to Professor David J. T. Hill on the occasion of his 75th birthday.

REFERENCES

1. Siegfried, D. L.; Thomas, D. A.; Sperling, L. H. In Polymer Alloys II; Klempner, D., Frisch, K. C., Eds.; Plenum Press: New York, 1980; pp 167–184.
2. Sperling, L. H. In Multicomponent Polymer Materials, ACS Advances in Chemistry Series 211; Paul, D. R., Sperling, L.

H., Eds.; American Chemical Society: Washington, DC, 1986; pp 21–56.
3. Sperling, L. H. In Interpenetrating Polymer Networks, ACS Advances in Chemistry Series 239; Klempner, D.; Sperling, L. H., Utracki, L. A., Eds.; American Chemical Society: Washington, DC, 1994; pp 3–38.
4. Sperling, L. H.; Mishra, V. Polym Adv Technol 1996, 7, 197.
5. Sperling, L. H. Polymeric Multicomponent Materials—An Introduction; Wiley: New York, 1997; (a) pp 335–381, (b) pp 24–29.
6. Jones, R. G.; Kahovec, J.; Stepto, R.; Wilks, E. S.; Hess, M.; Kitayama, T.; Metanomski, W. V. Compendium of Polymer Terminology and Nomenclature—IUPAC Recommendations 2008; RSC Publishing-IUPAC: Cambridge, UK, 2009; pp 188–189, 222, 386.
7. Staudinger, H. Ber Deut Chem Ges 1920, 53, 1073.
8. Staudinger, H.; Fritschi, J. Helv Chim Acta 1922, 5, 785.
9. Staudinger, H. Ber Deut Chem Ges 1926, 59, 3019.
10. Aylsworth, J. W. (Condensite Co.). U. S. Pat. 1,111,284 (1914).
11. Ostromislensky, I.; Shepard, M. G. (Naugatuck Chem. Co.). U. S. Pat.1,683,401 (1924).
12. Vernon, L. B.; Vernon, H. M. (Vernon-Benshoff Co.). U. S. Pat.2,234,993 (1941).
13. Staudinger, J. J. P.; Hutchinson, H. M. (The Distillers Co. Ltd). U. K. Pat.572,670 (1945).
14. Staudinger, J. J. P.; Hutchinson, H. M. (The Distillers Co. Ltd). U. S. Pat.2,539,376 (1951).
15. Staudinger, J. J. P.; Hutchinson, H. M. (The Distillers Co. Ltd). U. S. Pat.2,539,377 (1951).
16. Millar, J. R. J Chem Soc 1960, 1311.
17. Shibayama, K.; Suzuki, Y. Rubber Chem Technol 1967, 40, 476.
18. Siegfried, D. L.; Manson, J. A.; Sperling, L. H. J Polym Sci Polym Phys Ed 1978, 16, 583.
19. Thiele, J. L.; Cohen, R. E. Polym Eng Sci 1979, 19, 284.
20. Chirila, T. V.; Vijayasekaran, S.; Horne, R.; Chen, Y. C.; Dalton, P. D.; Constable, I. J.; Crawford, G. J. J Biomed Mater Res 1994, 28, 745.
21. Chirila, T. V. Biomaterials 2001, 22, 3311.
22. Hicks, C. R.; Clayton, A. B.; Vijayasekaran, S.; Crawford, G. J.; Chirila, T. V.; Constable, I. J. Ophthalmol Plast Reconstr Surg 1999, 15, 326.
23. Hicks, C. R.; Morris, I. T.; Vijayasekaran, S.; Fallon, M. J.; McAllister, J.; Clayton, A. B.; Chirila, T. V.; Crawford, G. J.; Constable, I. J. Br J Ophthalmol 1999, 83, 616.
24. Chirila T. V.; Constable, I. J.; Crawford, G. J.; Russo, A. V. (Lions Eye Institute). U. S. Pat.5,458,819 (1995).
25. Hicks, C.; Clayton, A.; Chirila, T.; Crawford, G.; Constable, I.; Fitton, J. (Lions Eye Institute). U. S. Pat.6,346,121 (2002).
26. Chirila, T. V.; Lou, X.; Vijayasekaran, S.; Ziegelaar, B. W.; Hong, Y.; Clayton, A. B. Int J Polym Mater 1998, 40, 97.
27. Chirila, T. V.; Hill, A. J.; Richens, D. T. Aust J Chem 2007, 60, 439.
28. Tighe, B.; Franklin, V. In The Eye in Contact Lens Wear, 2nd ed.; Larke, J. R., Ed.; Butterworth/Heinemann: Boston, 1997; pp 49–100.
29. Werner, L. In Biomaterials and Regenerative Medicine in Ophthalmology; Chirila, T., Ed.; Woodhead Publishing: Cambridge, UK, 2010; pp 35–64.
30. Hicks, C. R.; Chirila, T. V.; Werner, L.; Crawford, G. J.; Apple, D. J.; Constable, I. J Clin Exp Ophthalmol 2004, 32, 185.
31. Lee J. H.; Kim, S. L. Polym J 1984, 16, 453.
32. Klempner, D.; Frisch, K. C.; Xiao, X. H.; Frisch, H. L. Polym Eng Sci 1985, 25, 488.
33. Klempner, D.; Frisch, K. C.; Xiao, X. H.; Cassidy, E.; Frisch, H. L. In Multicomponent Polymer Materials, ACS Advances in Chemistry Series 211; Paul, D. R., Sperling, L. H., Eds.; American Chemical Society: Washington, DC, 1986; pp 211–230.
34. Hourston, D. J.; Schäfer, F. U.; Bates, J. S. J Appl Polym Sci 1996, 60, 2409.
35. Lou, X.; Vijayasekaran, S.; Chirila, T. V.; Maley, M. A. L.; Hicks, C. R.; Constable, I. J. J Biomed Mater Res 1999, 47, 404.
36. Kansy, J. Nucl Instrum Methods Phys Res A 1996, 374, 235.
37. Xie, W.; Ju, H.; Geise, G.; Freeman, B. D.; Mardel, J. I.; Hill, A. J. Macromolecules 2011, 44, 4428.
38. Nielsen, L. E.; Landel, R. F. Mechanical Properties of Polymers and Composites, 2nd ed.; CRC Press: Boca Raton, USA, 1994; pp 16–23.
39. Krause, S.; Gormley, J. J.; Roman, N.; Shetter, J. A.; Watanabe, W. H. J Polym Sci Part A: Gen Pap 1965, 3, 3573.
40. Haldon, R. A.; Simha, R. J Appl Phys 1968, 39, 1890.
41. Ilavský, M.; Hasa, J. Collect Czech Chem Commun 1968, 33, 2142.
42. Ilavský, M.; Hasa, J.; Janáček, J. Collect Czech Chem Commun 1968, 33, 3197.
43. Ilavský, M.; Hasa, J. Collect Czech Chem Commun 1969, 34, 2199.
44. Lednický, F.; Janáček, J. J Macromol Sci Phys 1971, 5, 335.
45. Kolařík. J.; Janáček, J. J Appl Polym Sci 1976, 20, 841.
46. Russell, G. A.; Gregonis, D. E.; DeVisser, A. A.; Andrade, J. D.; Dalling, D. K. In Hydrogels for Medical and Related Applications, ACS Symposium Series 31; Andrade, J. D., Ed.; American Chemical Society: Washington, DC, 1976; pp 139–150.
47. Kolařík, J. Adv Polym Sci 1982, 46, 119.
48. Roorda, W. E.; Bouwstra, J. A.; de Vries, M. A.; Junginger, H. E. Pharm Res 1988, 5, 722.
49. Hopfinger, A. J.; Koehler, M. G.; Pearlstein, R. A. J Polym Sci Part B: Polym Phys 1988, 26, 2007.
50. Goh, S. H.; Siow, K. S. Polym Bull 1990, 23, 205.
51. Di Marco, G.; Lanza, M.; Pieruccini, M. Nuovo Cimento 1994, 16D, 849.
52. Sun, Y.-M.; Lee, H. L. Polymer 1996, 37, 3915.
53. Kataoka, K.; Ito, H.; Amano, H.; Nagasaki, Y.; Kato, M; Tsuruta, T. J Biomater Sci Polym Ed 1998, 9, 111.
54. Hodge, R. M.; Simon, G. P.; Whittaker, M. R.; Hill, D. J. T.; Whittaker, A. K. J Polym Sci Part B: Polym Phys 1998, 36, 463.
55. Çaykara, T.; Özyürek, C.; Kantoğlu, Ö.; Erdoğan, B. Polym Degrad Stab 2003, 80, 339.
56. Meakin, J. R.; Hukins, D. W. L.; Imrie, C. T.; Aspden, R. M. J Mater Sci Mater Med 2003, 14, 9.
57. Gates, G.; Harmon, J. P.; Ors, J.; Benz, P. Polymer 2003, 44, 207.
58. Karabanova, L. V.; Boiteux, G.; Gain, O.; Seytre, G.; Sergeeva, L. M.; Lutsyk, E. D. Polym Int 2004, 53, 2051.
59. Salmerón Sánchez, M.; Touzé, Y.; Saiter, A.; Saiter, J. M.; Gómez Ribelles, J. L. Colloid Polym Sci 2005, 283, 711.
60. Li, S.; Shah, A.; Hsieh, A. J.; Haghighat, R.; Praveen, S. S.; Mukherjee, I.; Wei, E.; Zhang, Z.; Wei, Y. Polymer 2007, 48, 3982.
61. Karabanova, L. V.; Boiteux, G.; Seytre, G.; Stevenson, I.; Lloyd, A. W.; Mikhalovsky, S. V.; Helias, M.; Sergeeva, L. M.; Lutsyk, E. D.; Svyatyna, A. Polym Eng Sci 2008, 9, 588.
62. Vargün, E.; Usanmaz, A. J Macromol Sci Pure Appl Chem 2010, A47, 882.
63. Ribeiro, A.; Veiga, F.; Santos, D.; Torres-Labandeira, J. J.; Concheiro, A.; Alvarez-Lorenzo, C. Biomacromolecules 2011, 12, 701.
64. Kemal, E.; Adesanya, K. O.; Deb, S. J Mater Chem 2011, 21, 2237.
65. McCrum, N. G.; Read, B. E.; Williams, G. Anelastic and Dielectric Effects in Polymeric Solids; Wiley: New York, 1967; pp 141–144.
66. Heijboer, J. Int J Polym Mater 1977, 6, 11.
67. Williams, G. Adv Polym Sci 1979, 33, 60.
68. Zorn, R. J Phys: Condens Matter 2003, 15, R1025.
69. Deutsch, K.; Hoff, E. A. W.; Reddish, W. J Polym Sci 1954, 13, 565.
70. Hoff, E. A. W.; Robinson, D. W.; Willbourn, A. H. J Polym Sci 1955, 18, 161.
71. Mikhailov, G. P. J Polym Sci 1958, 30, 605.
72. Williams, G. Trans Faraday Soc 1966, 62, 2091.

73. Kolařík, J. J Macromol Sci Phys 1971, B5, 355.
74. Diaz Calleja, R. J Polym Sci Polym Phys Ed 1979, 17, 1395.
75. Bergman, R.; Alvarez, F.; Alegria, A.; Colmenero, J. J Chem Phys 1998, 109, 7546.
76. Alvarez, C.; Lorenzo, V.; Riande, E. J Chem Phys 2005, 122, 194905.
77. Janáček, J. J Macromol Sci Rev Macromol Chem 1973, C9, 1.
78. Li, B. Y.; Bi, X. P.; Zhang, D. H.; Wang, F. S. In Advances in Interpenetrating Polymer Networks; Klempner, D., Frisch, K. C., Eds.; Technomic: Lancaster, USA, 1989; Vol.I, pp 203–220.
79. Chung, G.-C.; Kornfield, J. A.; Smith, S. D. Macromolecules 1994, 27, 964.
80. Karabanova, L. V.; Lloyd, A. W.; Mikhalovsky, S. V.; Helias, M.; Phillips, G. J.; Rose, S. F.; Mikhalovska, L.; Boiteux, G.; Sergeeva, L. M.; Lutsyk, E. D.; Svyatyna, A. J Mater Sci Mater Med 2006, 17, 1283.
81. Karabanova, L. V.; Sergeeva, L. M.; Svyatyna, A. V.; Yakushev, P. N.; Egorova, L. M.; Ryzhov, V. A.; Bershtein, V. A. J Polym Sci Part B: Polym Phys 2007, 45, 963.
82. Dror, M.; Elsabee, M. Z.; Berry, G. C. Biomater Med Dev Artif Org 1979, 7, 31.
83. Prashantha, K.; Pai, K. V. K.; Sherigara, B. S.; Prasannakumar, S. Bull Mater Sci 2001, 24, 535.
84. Anžlovar, A.; Žigon, M. Acta Chim Slov 2005, 52, 230.
85. Davis, P. A.; Nicolais, L.; Ambrosio, L.; Huang, S. J. J Bioact Compat Polym 1988, 3, 205.
86. Eschbach, F. O.; Huang, S. J. In Interpenetrating Polymer Networks, ACS Advances in Chemistry Series 239; Klempner, D., Sperling, L. H., Utracki, L. A., Eds.; American Chemical Society: Washington, DC, 1994; pp 205–219.
87. Eschbach, F. O.; Huang, S. J. J Bioact Compat Polym 1994, 9, 29.
88. Jones, D. S.; McLaughlin, D. W. J.; McCoy, C. P.; Gorman, S. P. Biomaterials 2005, 26, 1761.
89. Giordano, C.; Causa, F.; Di Silvio, L.; Ambrosio, L. J Mater Sci Mater Med 2007, 18, 653.
90. Araújo, N.; Gomes, D.; Gómez Ribelles, J. L.; Monleón Pradas, M.; Mano, J. F. Polym Eng Sci 2006, 46, 930.
91. Zhao, J.; Xiao, C.; Xu, N.; Feng, Y. Polym Plast Technol Eng 2011, 50, 818.
92. Wang, J.; Li, X. J Appl Polym Sci 2011, 121, 3347.
93. Gloria, A.; De Santis, R.; Ambrosio, L.; Causa, F.; Tanner, K. E. J Biomater Appl 2011, 25, 795.
94. Murayama, S.; Kuroda, S.; Osawa, Z. Polymer 1993, 34, 2845.
95. Shi, S.; Kuroda, S.; Kubota, H. Materiaru Raifu Gakkaishi [J Mater Life Soc (Japan)] 2003, 15, 31.
96. Ramaraj, B.; Radhakrishnan G. Polymer 1994, 35, 2167.
97. Gursel, I.; Balcik, C.; Arica, Y.; Akkus, O.; Akkas, N.; Hasirci, V. Biomaterials 1998, 19, 1137.
98. Kayaman-Apohan, N.; Baysal, B. M. Macromol Chem Phys 2001, 202, 1182.
99. Bajpai, A. K.; Shrivastava, M. J Macromol Sci Pure Appl Chem 2002, A39, 667.
100. Kwok, A. Y.; Qiao, G. G.; Solomon, D. H. Chem Mater 2004, 16, 5650.
101. Abbasi, F.; Mirzadeh, H. Int J Adhes Adhes 2004, 24, 247.
102. Hatakeyama, T.; Nakamura, K.; Hatakeyama, H. Thermochim Acta 1988, 123, 153.
103. Hatakeyama, H.; Hatakeyama, T. Thermochim Acta 1998, 308, 3.
104. Jovanović, J.; Adnadjević, B.; Ostojić, S.; Kićanović, M. Mater Sci Forum 2004, 453–454, 543.
105. Sung, Y. K.; Gregonis, D. E.; Jhon, M. S.; Andrade, J. D. J Appl Polym Sci 1981, 26, 3719.
106. Nakanishi, H.; Wang, S. J.; Jean, Y. C. Positron Annihilation Studies of Fluids; World Science: Singapore, 1988; p 292.
107. Tao, J. J Chem Phys 1972, 56, 5499.
108. Eldrup, M.; Lightbody, D.; Sherwood, J. N. Chem Phys 1981, 63, 51.
109. Hill, A. J. In Polymer Characterization Techniques and Their Applications to Blends; Simon G. P., Ed.; Oxford University Press: Oxford, 2003; pp 401–435.
110. Burdon, J.; Oner, M.; Calvert, P. Mater Sci Eng C 1996, 4, 133.
111. Calvert, P.; Rieke, P. Chem Mater 1996, 8, 1715.
112. Taguchi, T.; Shirogawa, M.; Kishida, A.; Akashi, M. J Biomater Sci Polym Ed 1999, 10, 19.
113. Chirila, T. V.; Morrison, D. A.; Hicks, C. R.; Gridneva, Z.; Barry, C. J.; Vijayasekaran, S. Cornea 2004, 23, 620.
114. Chirila, T. V.; Morrison, D. A.; Gridneva, Z.; Meyrick, D.; Hicks, C. R.; Webb, J. M. Contact Lens Anter Eye 2005, 28, 21.
115. Zainuddin; Hill, D. J. T.; Chirila, T. V.; Whittaker, A. K.; Kemp, A. Biomacromolecules 2006, 7, 1758.
116. Chirila, T. V.; Zainuddin; Hill, D. J. T.; Whittaker, A. K.; Kemp, A. Acta Biomater 2007, 3, 95.
117. Chirila, T. V.; Zainuddin. React Funct Polym 2007, 67, 165.
118. Costa, R. O. R.; Pereira, M. M.; Lameiras, F. S.; Vasconcelos, W. L. J Mater Sci Mater Med 2005, 16, 927.
119. Chirila, T. V.; Gridneva, Z.; Morrison, D. A.; Barry, C. J.; Hicks, C. R.; Hill, D. J. T.; Whittaker, A. K.; Zainuddin. J Mater Sci 2004, 39, 1861.
120. Zainuddin; Chirila, T. V.; Hill, D. J. T.; Whittaker, A. K. J Mol Struct 2005, 739, 199.
121. Chirila, T. V.; Morrison, D. A.; Gridneva, Z.; Garcia, A. J. A.; Platten, S. T.; Griffin, B. J.; Zainuddin; Whittaker, A. K.; Hill, D. J. T. J Mater Sci 2005, 40, 4987.
122. Golomb, G.; Wagner, D. Biomaterials 1991, 12, 397.
123. Golomb, G.; Barashi, A.; Wagner, D.; Nachmias, O. Clin Mater 1993, 13, 61.
124. Hristov, H. A.; Bolan, B.; Yee, A. F.; Xie, L.; Gidley, D. W. Macromolecules 1996, 29, 8507.
125. Ghi, P. Y.; Hill, D. J. T.; Whittaker, A. K. Biomacromolecules 2002, 3, 991.
126. Vercoe, K. M.; Blakey, I.; Chirila, T. V.; Hill, A. J.; Whittaker, A. K. In New Approaches in Biomedical Spectroscopy, ACS Symposium Series 963; Kneipp, K., Aroca, R., Kneipp, H., Wentrup-Byrne, E., Eds.; American Chemical Society: Washington, DC, 2007; pp 391–409.
127. Ju, H.; McCloskey, B. D.; Sagle, A. C.; Wu, Y. H.; Kusuma, V. A.; Freeman, B. D. J Membr Sci 2008, 307, 260.
128. Ju, H.; Sagle, A. C.; Freeman, B. D.; Mardel, J. I.; Hill, A. J. J Membr Sci 2010, 358, 131.